Published in final edited form as:
Biol Cell. ; 102(3): 173–189. doi:10.1042/BC20090091.

TLRR (lrrc67) interacts with PP1 and is associated with a cytoskeletal complex in the testis

Rong Wang, **Aseem Kaul**, and **Ann O. Sperry**[§]
Department of Anatomy and Cell Biology, Brody School of Medicine at East Carolina University, Greenville, NC 27834 USA

Abstract

Background Information—Spermatozoa are formed via a complex series of cellular transformations, including acrosome and flagellum formation, nuclear condensation and elongation, and removal of residual cytoplasm. Nuclear elongation is accompanied by formation of a unique cytoskeletal structure, the manchette. We identified previously a leucine-rich repeat protein we named TLRR associated with the manchette that contains a protein phosphatase-1 binding site. Leucine-rich repeat proteins often mediate protein-protein interactions, therefore, we hypothesize that TLRR acts as a scaffold to link signaling molecules, including PP1, to the manchette near potential substrate proteins important for spermatogenesis.

Results—TLRR and PP1 interact with one another as demonstrated by coimmunoprecipitation and yeast 2-hybrid assay. TLRR binds more strongly to PP1γ2 than it does to PP1α. Anti-phosphoserine antibodies immunoprecipitate TLRR from testis lysate indicating that TLRR is a phosphoprotein. TLRR is part of a complex in testis that includes cytoskeletal proteins and constituents of the ubiquitin-proteasome pathway. The TLRR complex purified from 3T3 cells contains similar proteins, colocalizes with microtubules and is enriched at the microtubule-organizing center. TLRR is also detected near the centrosome of elongated, but not midstage, spermatids.

Conclusion—We demonstrate here that TLRR interacts with PP1, particularly the testis specific isoform, PP1γ2. Immunoaffinity purification confirms that TLRR is associated with the spermatid cytoskeleton. In addition, proteins involved in protein stability are part of the TLRR complex. These results support our hypothesis that TLRR links signaling molecules to the spermatid cytoskeleton in order to regulate important substrates involved in spermatid transformation. The translocation of TLRR from manchette to the centrosome region suggests a possible role for this protein in tail formation. Our finding that TLRR is associated with microtubules in cultured cells suggests that TLRR may play a common role in modulating the cytoskeleton in other cell types besides male germ cells.

Keywords

spermatogenesis; spermiogenesis; manchette; leucine-rich repeat; cytoskeleton; centrosome

Introduction

Formation of viable sperm entails a dramatic cytoskeletal rearrangement to transform a rather nondescript precursor cell into a polarized, elongated, free-swimming spermatozoon. During this developmental process, the acrosome forms, the nucleus condenses and elongates, the flagellum develops and the cytoplasm redistributes for eventual elimination as a residual body.

[§]Corresponding author AOS: sperrya@ecu.edu.

The manchette is a skirt-like structure comprised of a mantle of microtubules attached to a perinuclear ring that encircles the elongating spermatid nucleus during the period of its greatest morphological change (reviewed in Fawcett et al., 1971). The manchette is unique to the developing spermatid and demonstrates several forms of motility by constricting in diameter as it moves along the surface of the spermatid nucleus. In addition, both microtubules and microfilaments of the manchette act as tracks for the transport of vesicles to reallocate cytoplasmic contents for disposal during streamlining of the spermatid in the course of its maturation. Protein complexes are also conveyed along the manchette in a process termed intramanchette transport (IMT) thought responsible for the delivery of components to the centrosome and the sperm tail (reviewed in Kierszenbaum, 2002).

Consistent with the observed motility of the manchette, this structure contains both microtubule- and actin-based molecular motors. Kinesin molecular motors are associated with microtubules of the manchette including kinesin-1 (Hall et al., 1992), KIFC1 (a kinesin-13 member) (Yang and Sperry, 2003), and KIF17β (a kinesin-2 subfamily member) (Saade et al., 2007) as well as cytoplasmic dynein (Hall et al., 1992; Yoshida et al., 1994; Fouquet et al., 2000; Hayasaka et al., 2008). Myosin Va connects vesicles to microfilaments that are interspersed with microtubules of the manchette and is also found in the acroplaxome, a keratin-actin subacrosomal plate (Kierszenbaum et al., 2003; Hayasaka et al., 2008).

Besides molecular motors and cytoskeletal components, additional proteins have been localized to the manchette, an indication of its complex structure and function during spermiogenesis. Signaling molecules such as a testis-specific serine-threonine kinase and the fer tyrosine kinase have been found associated with manchette microtubules (Walden and Cowan, 1993; Walden and Millette, 1996; Tovich et al., 2004; Kierszenbaum et al., 2008). This placement of kinases is compatible with the proposal that the manchette provides an anchor for signaling molecules to regulate the cellular changes of spermiogenesis (Kierszenbaum, 2001). As expected, proteins involved in cellular remodeling and protein degradation are also linked to the manchette. CCT (cytoplasmic chaperonin containing TCP-1) is a chaperonin responsible for folding of α-and β-tubulin as well as actin and is highly expressed in the testis (Frydman et al., 1992; Gao et al., 1992; Yaffe et al., 1992; Kubota et al., 1999). CCT is localized to the spermatid manchette and to the centrosome but not to the sperm tail (Soues et al., 2003). The 26S proteasome is also found on the manchette, where it likely functions in degradation of cytoplasmic contents during spermatid remodeling (Rivkin et al., 1997; Mochida et al., 2000).

We have identified recently a leucine rich-repeat containing protein we have named TLRR (testis leucine rich repeat; also known as lrrc67, leucine rich repeat containing 67) that is highly expressed in the testis and localized near the transforming spermatid nucleus (Wang and Sperry, 2008). In addition to the leucine-rich repeats at its amino terminus, we found a consensus binding site for protein phosphatase-1 (PP1) in the carboxyl-terminal half of this protein (Wang and Sperry, 2008). We hypothesize that TLRR may participate in regulating the phosphorylation state of proteins near the spermatid nucleus by localizing PP1 to that site through its association with manchette microtubules. In this study, we demonstrate the binding of TLRR with PP1 through coimmunoprecipitation from testis lysates and yeast 2-hybid assays. TLRR in the testis exists in a multimeric complex containing cytoskeletal proteins as well as proteins important for protein folding and degradation including CCT and the 26S proteasome, known constituents of the manchette and centrosome in spermatids (Lange et al., 2000; Soues et al., 2003). In midstage spermatids, TLRR does not colocalize with γ-tubulin, however, TLRR redistributes to the centrosomal region in late state spermatids suggesting a possible role in tail formation. These data support our hypothesis that TLRR positions PP1 near the spermatid nucleus and places this regulatory protein near proteins important for spermiogenesis including those involved in cytoskeletal remodeling, trafficking, and protein degradation.

Materials and Methods

Co-immunoprecipitation

All use of animals was approved and conducted in accordance with the Guide for the Care and Use of Agricultural Animals in Agricultural Research and Teaching. Mouse testis extract was prepared as previously described (Zou et al., 2002). Briefly, decapsulated testes from adult mice were homogenized in buffer (10 mM MES, pH 6.75, 1 mM EGTA, 0.5 mM $MgCl_2$, 30% glycerol, 0.1% NP40) containing mammalian protease inhibitor cocktail (Sigma-Aldrich; St. Louis, MO), 3 μM PMSF and phosphatase inhibitor cocktail (Sigma-Aldrich; St. Louis, MO), centrifuged two times, first at 100,000xg and then 130,000xg, to remove cellular debris generating a high-speed supernatant fraction. Protein concentration in tissue lysates was determined by the Coomassie brilliant blue method (Bio-Rad; Hercules, CA). For coimmunoprecipitation experiments, affinity purified antibody to either TLRR or PP1γ2 was linked to CNBr activated Sepharose 4B (GE Healthcare; Pittsburgh, PA) according to manufacturer's instructions. Testis lysate (1.5–2 mg protein) was incubated with antibody-linked Sepharose beads overnight at 4°C. Immune complexes were collected by centrifugation, unbound protein removed, and the pellet washed extensively to remove nonspecifically bound protein. Bound proteins were then eluted from the pellet with triethanolamine (pH 11), denatured, proteins separated by SDS-PAGE and bound proteins detected by western blot. Negative control for coimmunoprecipitation with TLRR or PP1 antibodies was normal rabbit IgG (NRIgG) bound to beads. For experiments to determine whether TLRR or PP1γ2 are phosphorylated, testis extract was incubated with Sepharose beads linked to 12 μg anti-phosphoserine antibodies (mixture of clones 1CB, 4A3, 4A9, and 16B3 from EMD Chemical, Inc.; Gibbstown, NJ) or control beads linked to an equivalent amount of normal mouse IgG (NMIgG).

Yeast 2-Hybrid Analysis

Plasmids containing coding sequence for PP1γ1 and PP1γ2 were generous gifts of Dr. S. Vijayaraghavan, Kent State University. Both sequences were amplified by PCR before transfer into pGBKT7 using BamHI and EcoRI restriction sites engineered into the PCR primers. PP1γ1 was amplified with GAATTCGCGGATATCGACAAACTCAAC as the 5′ primer and GGATCCTTTCTTTGCTTGCTTTGTGATC as the 3′ primer while PP1γ2 was amplified with the same 5′ primer as for PP1γ1 and GGATCCCTCGTATAGGACCAGTGTTG as the 3′ primer. PP1α cloned into pGBKT7 was a kind gift of Dr. Susannah Varmuza, University of Toronto. Full-length TLRR cloned into pADT7 and the deletion construct TLRRA containing only the first 135 amino acids of TLRR and lacking the KVIF consensus binding site for PP1 were described previously (Wang and Sperry, 2008). The bait (PP1) and prey (TLRR) plasmids were cotransformed into yeast strain AH109 and activation of the LacZ and HIS3 reporter genes was determined by growth on selective plates containing X-α-Gal as described (Zhang et al., 2007). The yeast strain AH109 (Clontech; Palo Alto, CA) cotransformed with pGADT7-T and pGBKT7-53 was used as positive control for protein-protein interaction while cells containing pGADT7-T and pGBKT7-Lam, expressing proteins that do not interact, were negative controls for these experiments.

Western Blot

Protein samples from immunoprecipitation experiments or affinity purification fractions were separated by polyacrylamide gel electrophoresis (PAGE) through 10% acrylamide gels or precast 8–16% acrylamide gels (Invitrogen; Carlsbad, CA), equilibrated in and electrophoretically transferred from the gel matrix to PVDF membrane (Bio-Rad Laboratories; Hercules CA) in Towbin transfer buffer. Proteins were detected on the membrane with affinity purified TLRR antibody prepared as previously described at a dilution of 1:5,000 (Wang and Sperry, 2008). Other antibodies used for western blot in these experiments were the pan-PP1

antibodies PP1FL18 and PP1E9 (both at 1:250; Santa Cruz Biotechnology, Inc, Santa Cruz, CA), anti-PP1γ2 (1:5,000; kind gift of Dr. S. Vijayaraghavan, Kent State University) (Vijayaraghavan et al., 1996), anti-β-tubulin (1:1000; Sigma Aldrich, St. Louis, MO), anti-actin (20–33, Sigma Aldrich, St. Louis, MO), UIC 81 specific for kinesin-1B (1:250, kind gift of Dr. S. Brady, University of Illinois, Chicago) (DeBoer et al., 2008), anti-actin (20–33) (1:200; Sigma Aldrich, St. Louis, MO), IC 74.1 specific for one of the intermediate chains of dynein (1:250, kind gift of Dr. K. Pfister, University of Virginia) (Dillman and Pfister, 1994). Immune complexes bound to the membrane were detected with horseradish peroxidase-conjugated donkey secondary antibody (Jackson ImmunoResearch Inc.; West Grove, PA) diluted 1:40,000 in TTBS (100 mM Tris, pH 7.5, 150 mM NaCl, 0.1% Tween 20) and developed with enhanced chemiluminescent reagents as described by the manufacturer (GE Healthcare; Pittsburgh, PA).

Immunoaffinity Purification

A concentrated TLRR antibody stock (about 5 mg/ml) was prepared by affinity purification using the antigenic peptide linked to CNBr activated Sepharose 4B according to manufacturer's instructions. An affinity purification column was prepared essentially according to the method of Huang et al. (2002) adapted from Ausubel (1987). The 1 ml column was equilibrated in ice-cold TSA buffer (10 mM Tris-HCl, pH 8.2, 140 mM NaCl, .025% $NaNa_3$) supplemented with protease and phosphatase inhibitors. Approximately 20–50 mg testis lysate in 1.0 ml TSA was loaded onto the column and incubated, with gentle mixing, overnight at 4°C. The column was then washed sequentially with 5 bed volumes of each of the following buffers: wash 1 (10 mM Tris, pH 8.0, 140 mM NaCl, 0.5% Triton X-100, 0.5% sodium deoxycholate), wash 2 (50 mM Tris, pH 8.0, 0.5 M NaCl, 0.1% Triton X-100) and wash 3 (50 mM Tris, pH 9.0, 0.5 M NaCl, 0.1% Triton X-100) and the flow-through collected. Bound complexes were eluted from the column with 2.5 ml elution buffer (50 mM triethanolamine, pH 11.5, 0.1% Triton X-100, 0.15 M NaCl) and fractions immediately neutralized with 1 M Tris, pH 6.7. A parallel negative control column was prepared with an equal amount of nonspecific antibody (normal rabbit IgG) linked to Sepharose and loaded and eluted identically to the experimental sample. Column eluates were concentrated 20–30 fold on an Amicon ultra-4 filter unit (Millipore; Billerica, MA) prior to analysis by SDS-PAGE.

Proteomic Analysis

Proteins eluted from affinity columns were separated by electrophoresis on precast 8–16% acrylamide gels (Invitrogen; Carlsbad, CA). Gels were fixed in 25% isopropanol/10% acetic acid for 20 minutes, stained with 0.01% Coomassie R-250 (Bio-Rad; Hercules, CA), and destained with 10% acetic acid. Stained bands, not present in the negative control, were excised and proteins digested in gel with trypsin and identified by MALDI-TOF/TOF and MALDI mass fingerprinting and database search by the UNC-Duke Michael Hooker Proteomics Center (University of North Carolina-Chapel Hill). Kinesin-1 sequences (1A accession number NM_008447, 1B accession number NM_008448, and 1C accession number NM_008449) were aligned using the clustalW2 alignment software (Larkin et al., 2007) and printout prepared using the Boxshade program.

Colocalization

TLRR was detected in cultured cells essentially as previously described (Yang and Sperry, 2003). COS7 cells were grown to approximately 70% confluence on coverslips, fixed and permeabilized with a 50:50 mixture of acetone:methanol or straight methanol at −20°C for 10 minutes, and blocked in 2% BSA in TBST (20 mM Tris, pH 7.5, 154 mM NaCl, 2 mM EGTA, 2 mM $MgCl_2$, 0.1% Triton X-100) for 30 minutes. The cells were incubated with TLRR polyclonal antibody diluted 1:50 in TBST (approximately 100 μg/ml) overnight at 4°C. The

TLRR polyclonal antibody was detected with a Texas Red-conjugated donkey anti-rabbit IgG secondary antibody (1:100 dilution; Jackson ImmunoResearch Laboratories; West Grove, PA) and tubulin detected with a FITC-conjugated monoclonal anti-α-tubulin antibody (1:200; Sigma Aldrich; St. Louis, MO). DNA was stained with DAPI incorporated into Vectashield mounting media (Vector Laboratories; Burlingame, CA). In certain experiments, 2.5 μg/ml nocodazole was added to culture media in order to depolymerize microtubules. After 1.5 hours of treatment, the media was replaced with fresh media lacking nocodazole, incubated for 1, 2, or 3 hours, and the cells fixed and double-stained for TLRR and tubulin as described above.

For colocalization in testis sections, testes obtained from sexually mature mice were immersion fixed overnight in 4% paraformaldehyde (PFA) in phosphate buffered saline (PBS, pH 7.4) after piercing of the capsule. The organs were then incubated overnight in 0.5 M sucrose in PBS, placed in cryoprotectant, cut into 10μm sections, transferred to Vectabond coated slides (Vector Laboratories; Burlingame, CA), quickly dipped in −20°C acetone, and allowed to dry. The sections were washed with PBS and treated with 0.3% Triton X-100 for 15 minutes at room temperature. The tissue was blocked in 2% BSA in TBST and incubated with TLRR polyclonal antibody diluted 1:50 in TBST and anti-γ-tubulin diluted 1:50 (clone GTU-88, Sigma-Aldrich; St. Louis, MO). TLRR was detected as described above for colocalization in cultured cells and γ-tubulin detected with mouse anti-γ-tubulin conjugated to FITC (1:100 dilution; Jackson ImmunoResearch Laboratories; West Grove, PA). The intracellular localization of proteins was observed with a Nikon E600 fluorescence microscope, Pan Fluor 100X objective (N.A. 0.5–1.3), fit with appropriate filters and images captured with an Orca II CCD camera, model C4742-95 (Hamamatsu, Bridgewater, NJ) and Metamorph image analysis and acquisition software (Universal Imaging Corporation, Downingtown, PA). Images were exported to Photoshop and only linear adjustments to brightness and/or contrast were performed.

Results

TLRR interacts with Protein Phosphatase-1 in testis

We previously identified a short amino acid sequence, KVIF, in the carboxyl half of TLRR that matches the consensus binding site for PP1, $(R/K)x_1(V/I)x_2(F/W)$ (Wang and Sperry, 2008). In order to determine whether these two proteins interact in the testis, we performed coimmunoprecipitation studies in testis lysates. Two antibodies that recognize all isoforms of PP1, PP1E9 and PP1FL18, were able to coimmunoprecipitate TLRR (Figure 1A and B). In addition, an antibody specific for the γ2 isoform of PP1 found only in the testis also coimmunoprecipitates TLRR (Figure 1C). In each case a fraction of total TLRR in the testis is complexed with PP1 (compare Sn, representing unbound protein, to IP, corresponding to protein bound to PP1, in each panel). In turn, the TLRR antibody is able to coimmunoprecipitate PP1γ2 (Figure 1D); however, the percentage of total PP1γ2 associated with TLRR in the adult testis is very small. The negative control with normal rabbit IgG linked to beads did not precipitate the target proteins.

These data strongly suggest that a portion of cellular TLRR exists in the same complex as PP1 but does not establish whether the interaction is direct. In order to explore this possibility, we conducted yeast 2-hybrid experiments using yeast expressing full-length TLRR (TLRRFL) in combination with the PP1 isoforms PP1α, PP1γ1, and PP1γ2 (Figure 1E). Colonies containing TLRRFL and PP1γ2 (Figure 1E k, l) were blue on selective plates, indicating that these proteins do interact directly with one another. However, their growth was not nearly as robust as that of positive control colonies (Figure 1E g, o) indicating either that the interaction between these two proteins is weak or that expression of TLRRFL and/or PP1 inhibits yeast growth. It has been shown previously that PP1 overexpression is deleterious to yeast growth (Liu et al., 1992); the possibility that TLRR might modulate this effect is currently under investigation.

Yeast coexpressing TLRRFL and PP1γ1 (Figure 1E e, f) were less positive than the TLRRFL/PP1γ2 cotransformants but distinctly more so compared to cotransformants with PP1α which were entirely white on indicator plates (Figure 1E a, b). These results suggest that interaction between TLRR and PP1 is specific for the gamma isoforms and is strongest with PP1γ2. Surprisingly, the TLRR construct containing only the first 135 amino acids (TLRRA) and lacking the potential PP1 binding site also appeared blue on indicator plates when cotransformed with PP1 (Figure 1E i, j, m, n).

TLRR is likely a phosphoprotein

Because TLRR interacts with PP1, we wanted to determine whether it is a candidate substrate for PP1. TLRR contains 12 serine residues with an extremely high probability of phosphorylation using phosphorylation prediction software and only 2 threonine residues with a modest probability of phosphorylation (Blom et al., 1999) (Supplementary Data, Figure 1A). Most of the serine residues (9 out of 12) are located in the carboxyl half of the molecule where the PP1 binding site is situated (Supplementary Data, Figure 1B).

To test whether TLRR might be serine phosphorylated in the testis, we immunoprecipitated proteins from testis lysate using anti-phosphoserine specific antibodies and probed the immunoprecipitate with the TLRR antibody (Figure 2A, upper panel). A portion of total testicular TLRR is immunoprecipitated with anti-phosphoserine antibodies making it a potential substrate for PP1 in the testis. When this same blot was probed with the PP1γ2 specific antibody, no signal was detected in the immunoprecipitate, even after over exposure (Figure 2A, lower panel) suggesting that PP1γ2 is not phosphorylated in testis lysate at the level of detection afforded by these antibodies and/or PP1γ2 that is associated with TLRR is unphosphorylated. The negative control with normal mouse IgG linked to beads did not precipitate TLRR or PP1γ2 from testis lysate.

We performed the complementary experiment by immunoprecipitating either TLRR (Figure 2B) or PP1γ2 (Figure 2C) from testis lysate and probing the blots with the anti-phosphoserine antibody. In general, the TLRR IP displayed a greater number of reactive bands when compared to the PP1γ2 IP indicating that the TLRR complex may contain a number of phosphorylated proteins. In addition, we confirmed that the target proteins were immunoprecipitated by reprobing each blot with the corresponding immunprecipitating antibody. Immunoprecipitated TLRR reacts with the phosphoserine antibody (arrow, 2B) while immunoprecipitated PP1γ2 does not (upper panel, 2C). These data confirm our results above that TLRR is a phosphoprotein in testis lysate. In addition, neither TLRR nor PP1γ2 appears phosphorylated in immunoprecipitates with the partner protein although this is difficult to discern with regard to PP1γ2 coimmunoprecipitated with TLRR because of the relatively high background of the TLRR IP blot.

Proteomic analysis of TLRR complex

TLRR is found near the spermatid manchette in developing spermatids (Wang and Sperry, 2008); therefore, we reasoned that this protein might be part of a cytoskeletal complex. We conducted a proteomic analysis of the TLRR complex in the testis in an effort to understand the role of TLRR in this tissue. Proteins associated with TLRR were purified from testis lysate using our affinity-purified TLRR antibody linked to Sepharose beads. Bound proteins were eluted from the column, resolved by PAGE and stained with Coomassie (Figure 3). Fifteen protein bands that specifically bound to the TLRR antibody column when compared to a control column crosslinked to normal rabbit IgG were excised from the gel, sequenced, and compared to protein databases. The identified proteins purified with the TLRR antibody can be divided roughly into 3 categories: cytoskeletal components (Table 1A), proteins important for regulating protein stability (Table 1B), or miscellaneous metabolic enzymes and other proteins

(Table 1C). Each table displays the significant matches ($p<0.05$) in order of percent sequence coverage and number of peptides identified for each protein.

β-tubulin, and α-, β-, and γ-actin, subunits of cytoskeletal polymers, were purified with the TLRR antibody (Figure 3, bands 7, 1 and 5). In addition to the microtubule-based motor kinesin-1B, actin-based motors are also associated with the TLRR complex. Three isoforms of non-muscle myosin heavy chain, myh11, myh10, and myh9, were affinity purified with TLRR (Figure 3, band 15). The regulatory light chain 9 is also part of the complex (Figure 3, band 1).

The largest category of proteins associated with TLRR participates in either protein folding or protein degradation (Table 1B). These include 3 subunits of the CCT (chaperonin containing TCP-1) complex involved in folding of tubulin and actin subunits (Figure 3, bands 8 and 9) (Gao et al., 1992;Yaffe et al., 1992), and heat shock proteins hsp90 and hsp4-like (a member of the hsp70 family). Another well represented group associated with the TLRR complex participates in protein degradation including three regulatory subunits of the 26S proteasome (subunit 1, 2, and 3, Figure 3 bands 13, 11, and 8) and VCP (vasolin-containing peptide), required for ubiquitin-proteasome mediated protein degradation (Dai and Li, 2001). Our data is consistent with those from other labs that localized both the proteasome and CCT to the spermatid manchette (Rivkin et al., 1997;Soues et al., 2003).

Kinesin-1B is associated with TLRR

Tubulin is found in the TLRR complex along with the microtubule-based motor kinesin-1B (Table 1A, Figure 3). Twenty-five peptides matched the kinesin-1B sequence (Table 1A), with some of these peptides overlapping (Supplementary Data, Figure 2). Kinesin-1B is one of 3 highly homologous isoforms of the kinesin-1 heavy chain expressed in the mouse with different tissue and developmental expression profiles (Aizawa et al., 1992;Vignali et al., 1997;Xia et al., 1998;Kanai et al., 2000;Cai et al., 2001). Therefore, we examined the sequence of the peptides and compared them to the published sequence of each isoform. Of the 25 peptides (overlines in Supplemental Data, Figure 2), 19 were exact matches to kinesin-1B sequence with mismatches compared to the A and C isoforms. The 6 sequences that share common sequences are indicated by an asterisk (Supplemental Data, Figure 2). This is strong evidence that TLRR interacts exclusively with the B isoform of kinesin-1 in testis and not with the A or C isoforms.

Confirmation of cytoskeletal interactions

Our proteomic analysis indicated that TLRR resides in a complex containing cytoskeletal polymer subunits and the molecular motor kinesin-1B (see Figure 3 and Table 1A). To confirm and extend these findings, we conducted coimmunoprecipitation experiments of TLRR with cytoskeletal proteins in testis lysates. First, we confirmed that our TLRR antibody could coimmunoprecipitate tubulin and actin from testis lysate, consistent with its localization near the spermatid manchette, a stable cytoskeletal structure composed of microtubules and microfilaments (Figure 4A and B). Our proteomic analysis (Table 1A) identified kinesin-1B as associated with TLRR and analysis of the peptides obtained from the tryptic digest (Supplemental Data, Figure 2) confirmed this result. We used an antibody prepared by Dr. Scott Brady (University of Illinois at Chicago) and his colleagues specific for the B isoform of kinesin-1, UIC 81, to demonstrate that TLRR can coimmunoprecipitate kinesin-1B from testis lysate (Figure 4C) (DeBoer et al., 2008). We also wanted to investigate whether dynein, a minus-end directed microtubule motor associated with the manchette (Hall et al., 1992;Yoshida et al., 1994;Fouquet et al., 2000;Hayasaka et al., 2008), is coimmunoprecipitated with the TLRR antibody from testis lysate. A fraction of the total population of the 74.1 intermediate chain of dynein in the testis is found associated with the TLRR antibody (Figure

4D). We also attempted to determine whether myosin Va, shown by others to be associated with the manchette (Kierszenbaum et al., 2003;Hayasaka et al., 2008), immunoprecipitates with TLRR using the dil2 antibody to myosin Va (kind gift of Dr. J.A. Mercer, McLaughlin Research Institute) (Rogers et al., 1999). However, our results were inconclusive perhaps because the level of myosin Va in total testis lysate could not be detected by western blot with this antibody (unpublished data).

TLRR is expressed in cultured cells in association with microtubules

In the process of transfection studies using TLRR expression vectors, we discovered that several cultured cell lines express the TLRR protein (Figure 5A). We then wanted to determine whether TLRR is associated with microtubules in cultured cells as it is in the testis. Such a finding would provide a malleable system for investigation of TLLR function in the future. TLRR localizes to the microtubule network in COS7 cells (and 3T3 cells, unpublished data) including the microtubule organizing center (MTOC) (Figure 5B). In many cells, we observed that TLRR stained a ring, or loop, around the center of the MTOC (arrowheads, panel a and b, Figure 5B). Interestingly, we observed that in cells that appeared motile, with a clearly defined leading edge (upper side of 5B, b′), TLRR along with the MTOC was oriented toward the leading edge and displaced from the nucleus (arrow, Figure 5B, b″).

In order to compare the protein composition of the TLRR complex in testis (Table 1) with that in cultured cells, we conducted a proteomic analysis of the complex purified from 3T3 cell lysate. In this experiment, 6 bands were excised from a gel containing proteins affinity purified from 3T3 cell lysate with the TLRR antibody and 10 proteins were identified in the complex (Supplementary Data, Table 1). The complexes purified from the two cell types contain numerous proteins in common including cytoskeletal proteins and members of the hsp70 and hsp90 family. In addition, both kinesin-1B and dynein intermediate chain 74.1 coimmunoprecipitated with the anti-TLRR antibody from 3T3 cell lysate (Supplementary Data, Figure 3). These data are consistent with a role for TLRR in the structure and/or regulation of the cytoskeleton.

TLRR is associated with the centrosome in late stage spermatids

TLRR localizes in part to the MTOC in cultured cells (this report) and to the nucleus of developing spermatids (arrowheads, Figure 6a; Wang and Sperry, 2008). We next wanted to determine whether the localization of TLRR correlates with the spermatid centriole. Therefore, testis sections were double stained with our TLRR antibody and an antibody to gamma tubulin. In midstage spermatids, TLRR is localized to the manchette (arrowheads, Figure 6a, a″) and does not appreciably colocalize with gamma tubulin (arrows, Figure 6a′, a″). However, in later stage spermatids, TLRR localizes to the centrosome region of the elongating spermatid (arrowheads, Figure 6b, b″). At this stage, we routinely observed a bright spot of gamma tubulin staining alongside an area of more diffuse staining (arrowheads, Figure 6b′). TLRR staining (arrowheads, Figure 6b″) typically appears just adjacent to the bright spot of gamma tubulin staining (arrows, Figure 6b″).

Nocodazole treatment does not completely disrupt TLRR localization

Because TLRR is associated with the microtubule cytoskeleton in cultured cells, we next wanted to determine whether TLRR localization is affected by microtubule depolymerization. COS7 cells were treated with nocodazole to depolymerize microtubules and then the drug removed and the cells allowed to recover from drug treatment. Representative fluorescent staining of cells for TLRR and tubulin after 0, 60, 120 and 180 minutes of recovery are shown in Figure 7. In treated cells without recovery, TLRR does not diffuse throughout the cytoplasm, as does tubulin, but remains filamentous in appearance (Figure 7b). In some cells, TLRR staining appeared highly localized at the MTOC (unpublished data); however overall

organization of TLRR appears more disorganized in treated compared to untreated cells (compare Figure 7b to 5B, a). At 1 hour of recovery from nocodazole, short microtubules are observed extending from the MTOC into the cytoplasm (arrows, inset Figure 7d) with TLRR still filamentous in appearance. By the time a normal array of microtubules is apparent at 3 hours of recovery, TLRR staining also displays its normal morphology with strong staining at the MTOC and radial staining along microtubules (Figure 7k). These data suggest that TLRR localization is not entirely dependent on microtubule polymerization.

Discussion

We have shown previously that TLRR is localized near the developing spermatid nucleus and contains 4 leucine rich repeats as well as a consensus binding site for protein phosphatase-1 (Wang and Sperry, 2008). In this manuscript we begin to test our hypothesis that TLRR links PP1 to the spermatid cytoskeleton in order to localize this enzyme near important cellular substrates involved in cellular transformation. To determine whether TLRR interacts with PP1 in the testis, we conducted coimmunoprecipitation experiments in testis lysates. Antibodies that recognize all isoforms of PP1, PP1E9 or PP1FL18, are able to immunoprecipitate the TLRR protein from testis lysate. In addition, we demonstrate that a portion of testicular TLRR is complexed with the testis-specific isoform of PP1, PP1γ2. Yeast 2-hybrid assays confirm this interaction and suggest that binding is not solely dependent on the KVIF motif because interaction still occurs when a TLRR fragment lacking this sequence is used. This is not unusual for PP1 regulatory proteins that often have regions of affinity for PP1 in addition to the consensus binding site (Cohen, 2002). Our interaction studies also indicate a preference for binding between TLRR and PP1γ2 compared to PP1α.

Our work is consistent with that of Vijayaraghavan and colleagues showing that PP1γ2, necessary for sperm motility, is also required for sperm maturation and is localized in developing spermatids as is TLRR (Chakrabarti et al., 2007). These findings along with our own support our hypothesis that TLRR, associated with the manchette, brings PP1 near this structure in developing spermatids. sds22, a homolog of TLRR, binds to and inhibits the activity of PP1γ2 in caudal, but not caput, spermatozoa (Mishra et al., 2003). The mechanism underlying this inhibition is uncertain; however, it has been proposed that sds22 binding to PP1γ2 is regulated by sds22 phosphorylation (Huang et al., 2002; Mishra et al., 2003). We demonstrate here that TLRR is likely a phosphoprotein and speculate that its phosphorylation may also regulate its binding to PP1.

TLRR is localized near the manchette of elongating spermatids, a structure rich in microtubules, microfilaments and associated motor proteins. Therefore, we anticipated that the protein complex associated with TLRR would contain cytoskeletal proteins. Our proteomic analysis, and coimmunoprecipitation experiments, revealed that both actin and tubulin are associated with the TLRR complex as well as both microtubule-based and actin-based molecular motors. Our results are similar to those of Cheng, et al. who recently identified a multimeric complex containing PP1γ2 and actin along with other proteins in mouse testis lysate (Cheng et al., 2009). However, PP1 was not identified in our proteomic analysis of the TLRR complex, indicating that its interaction may be transient or small compared to the proteins we detected. Alternatively, PP1 is highly resistant to trypsin digestion, possibly rendering it underrepresented in sequence analysis following tryptic digestion (Feng et al., 1991).

Peptide analysis demonstrated that only the B isoform of kinesin-1 is associated with the TLRR complex. Peptides exclusive to kinesin-1B, and not the A and C isoform were detected in the affinity-purified TLRR complex. This result could indicate either that the TLRR complex excludes the A and C isoforms by providing binding sites only for kinesin-1B or that neither A nor C isoforms are present in the cell types that express TLRR. Junco et al. (2001) were able

to detect all 3 kinesin-1 isoforms in the testis by RT-PCR, but only the kinesin-1C isoform in spermatids.

In addition, our coimmunoprecipitation experiments demonstrate that the minus-end directed motor dynein is associated with this complex. Our data that both plus-end and minus-end directed motors are associated with TLRR is consistent with immunofluorescent localization of these motors to the manchette by others and support the idea that the manchette transports cargo in both directions. The interaction of both PP1 and kinesin-1B with TLRR suggests a possible role for TLRR in regulation of kinesin-1B activity associated with the manchette. PP1 is an important regulator of kinesin-based vesicle motility by activation of glycogen synthase kinase-3β which then phosphorylates the light chain of kinesin releasing it from its cargo and inhibiting transport (Morfini et al., 2002). Kinesin represents a candidate target on the microtubule manchette for PP1 in association with TLRR.

One of the most intriguing findings from our experiments was the association of numerous nonregulatory subunits of the 26S proteasome with the TLRR complex. This result is consistent with previous immunolocalization of subunits of the proteasome to the spermatid manchette (Rivkin et al., 1997) and supports a role for the manchette in degradation of proteins during sperm maturation. Recently, the proteasome has been implicated in regulation of microtubule dynamics (Csizmadia et al., 2008; Didier et al., 2008; Poruchynsky et al., 2008), therefore, its localization on the manchette might facilitate a role for the proteasome in controlling the stability of the manchette itself. In addition to subunits of the 26S proteasome, we found hsp90 associated with the TLRR complex. This data is in accordance with work of others that demonstrate a requirement of Hsp90 for assembly and stabilization of the proteasome (Imai et al., 2003).

We previously identified TLRR in a testis cDNA library and demonstrated that it is highly expressed in the testis and localized near the cytoskeleton of developing spermatids (Wang and Sperry, 2008). In this paper we report that the TLRR protein is also expressed in many cell lines where it is closely aligned with the microtubule cytoskeleton including the MTOC. Proteomic and coimmunoprecipitation analysis of the TLRR complex in cultured cells revealed common components including cytoskeletal polymer subunits and heat shock proteins. However, we did not detect proteasome subunits or CCT in the complex from cultured cells indicting either that our analysis was incomplete or that these protein complexes are preferentially associated with TLRR in the testis. Our data suggest that TLRR may play a common role in cells that can be modulated in specialized cells types, for example in the stable manchette cytoskeletal structure present in developing spermatids.

The behavior of the centrosome during gametogenesis has been the focus of intense interest based upon the importance of establishing an intact spindle to support early divisions of the zygote. In many species, the male and female gametes provide a reciprocal contribution of pericentriolar material (male) and centriole (female) to reconstitute a functional centrosome after fertilization (Manandhar et al., 2005). In the mouse, however, the centrosome undergoes complete degeneration during spermatogenesis (Manandhar et al., 1998). Here we report that, although TLRR is found on cytoplasmic microtubules and near the MTOC in cultured cells, these proteins display a different distribution during male germ cell development. TLRR is closely associated with the manchette of mid-stage spermatids followed by relocation to the centrosomal region of the spermatid (Figure 6). The relocation of TLRR from the manchette to the centrosome has been observed for a number of other proteins (Kierszenbaum, 2002) including components of the ubiquitin proteasome system (Rivkin et al., 1997; Rivkin et al., 2009) which we have shown here to be part of the testis TLRR complex.

Expression profiling has recently identified TLRR as a predicted cilia-related gene based on overexpression in highly ciliated cell types such as lung, olfactory epithelium, trachea, testis, and vomeronasal organ (McClintock et al., 2008). In addition, this protein is part of the ciliome database (http://www.ciliome.com). This is consistent with our localization of this protein to the MTOC in cultured cells (Figures 5a, b and 7k) and near the centrosomal region in spermatids and supports a role for TLRR in microtubule organization and/or biogenesis of cilia/flagella.

The TLRR protein is closely associated with the developing spermatid nucleus. We demonstrate in this manuscript that TLRR interacts with PP1 and cytoskeletal proteins as well as proteins important for the regulation of protein stability and turnover. Our data support our previous immunolocalization of TLRR to the manchette and are consistent with our hypothesis that TLRR serves to link PP1, and other regulatory molecules, near the nucleus of developing male germ cells in order to guide proper cell transformation.

Supplementary Material

Refer to Web version on PubMed Central for supplementary material.

Acknowledgments

The authors would like to acknowledge the technical assistance of Nicole DeVaul.

Funding This work was supported by grants from the Division of Research and Graduate Studies, East Carolina University and from the National Institutes of Health (HD058027) to AOS.

Abbreviations used

TLRR	testis leucine-rich repeat
PP1	protein phosphatase-1
MTOC	microtubule organizing center
CCT	cytoplasmic chaperonin containing TCP-1
NRIgG	normal rabbit IgG
NMIgG	normal mouse IgG

References

Aizawa H, Sekine Y, Takemura R, Zhang Z, Nangaku M, Hirokawa N. Kinesin family in murine central nervous system. J. Cell Biol 1992;119:1287–1296. [PubMed: 1447303]

Ausubel, FM. Current Protocols in Molecular Biology. John Wiley and Sons, Inc.; New York: 1987.

Blom N, Gammeltoft S, Brunak S. Sequence and structure-based prediction of eukaryotic protein phosphorylation sites. J. Mol. Biol 1999;294:1351–1362. [PubMed: 10600390]

Cai Y, Singh BB, Aslanukov A, Zhao H, Ferreira PA. The docking of kinesins, KIF5B and KIF5C, to Ran-binding Protein 2 (RanBP2) is mediated via a novel RanBP2 domain. J. Biol. Chem 2001;276:41594–41602. [PubMed: 11553612]

Chakrabarti R, Kline D, Lu J, Orth J, Pilder S, Vijayaraghavan S. Analysis of Ppp1cc-null mice suggests a role for PP1gamma2 in sperm morphogenesis. Biol. Reprod 2007;76:992–1001. [PubMed: 17301292]

Cheng L, Pilder S, Nairn AC, Ramdas S, Vijayaraghavan S. PP1gamma2 and PPP1R11 Are Parts of a Multimeric Complex in Developing Testicular Germ Cells in which their Steady State Levels Are Reciprocally Related. PLoS ONE 2009;4:e4861. [PubMed: 19300506]

Cleveland DW, Lopata MA, MacDonald RJ, Cowan NJ, Rutter WJ, Kirschner MW. Number and evolutionary conservation of alpha- and beta-tubulin and cytoplasmic beta- and gamma-actin genes using specific cloned cDNA probes. Cell 1980;20:95–105. [PubMed: 6893015]

Cohen PT. Protein phosphatase 1--targeted in many directions. J Cell Sci 2002;115:241–256. [PubMed: 11839776]

Csizmadia V, Raczynski A, Csizmadia E, Fedyk ER, Rottman J, Alden CL. Effect of an experimental proteasome inhibitor on the cytoskeleton, cytosolic protein turnover, and induction in the neuronal cells in vitro. Neurotoxicology 2008;29:232–243. [PubMed: 18155769]

Dai RM, Li CC. Valosin-containing protein is a multi-ubiquitin chain-targeting factor required in ubiquitin-proteasome degradation. Nat. Cell Biol 2001;3:740–744. [PubMed: 11483959]

DeBoer SR, You Y, Szodorai A, Kaminska A, Pigino G, Nwabuisi E, Wang B, Estrada-Hernandez T, Kins S, Brady ST, Morfini G. Conventional kinesin holoenzymes are composed of heavy and light chain homodimers. Biochemistry 2008;47:4535–4543. [PubMed: 18361505]

Didier C, Merdes A, Gairin JE, Jabrane-Ferrat N. Inhibition of proteasome activity impairs centrosome-dependent microtubule nucleation and organization. Mol. Biol. Cell 2008;19:1220–1229. [PubMed: 18094058]

Dillman JF 3rd, Pfister KK. Differential phosphorylation in vivo of cytoplasmic dynein associated with anterogradely moving organelles. J. Cell Biol 1994;127:1671–1681. %R 10.1083/jcb.127.6.1671. [PubMed: 7528220]

Eddinger TJ, Wolf JA. Expression of four myosin heavy chain isoforms with development in mouse uterus. Cell Motil. Cytoskeleton 1993;25:358–368. [PubMed: 8402956]

Fawcett DW, Anderson WA, Phillips DM. Morphogenetic factors influencing the shape of the sperm head. Dev. Biol 1971;26:220–251. [PubMed: 5168310]

Feng ZH, Wilson SE, Peng ZY, Schlender KK, Reimann EM, Trumbly RJ. The yeast GLC7 gene required for glycogen accumulation encodes a type 1 protein phosphatase. J. Biol. Chem 1991;266:23796–23801. [PubMed: 1660885]

Fouquet J, Kann M, Soues S, Melki R. ARP1 in Golgi organisation and attachment of manchette microtubules to the nucleus during mammalian spermatogenesis. J. Cell Sci 2000;113(Pt 5):877–886. [PubMed: 10671377]

Frydman J, Nimmesgern E, Erdjument-Bromage H, Wall JS, Tempst P, Hartl FU. Function in protein folding of TRiC, a cytosolic ring complex containing TCP-1 and structurally related subunits. EMBO J 1992;11:4767–4778. [PubMed: 1361170]

Gao Y, Thomas JO, Chow RL, Lee GH, Cowan NJ. A cytoplasmic chaperonin that catalyzes beta-actin folding. Cell 1992;69:1043–1050. [PubMed: 1351421]

Gruppi CM, Zakeri ZF, Wolgemuth DJ. Stage and lineage-regulated expression of two hsp90 transcripts during mouse germ cell differentiation and embryogenesis. Mol. Reprod. Dev 1991;28:209–217. [PubMed: 2015079]

Gu W, Tekur S, Reinbold R, Eppig JJ, Choi YC, Zheng JZ, Murray MT, Hecht NB. Mammalian male and female germ cells express a germ cell-specific Y-Box protein, MSY2. Biol. Reprod 1998;59:1266–1274. [PubMed: 9780336]

Hall ES, Eveleth J, Jiang C, Redenbach DM, Boekelheide K. Distribution of the microtubule-dependent motors cytoplasmic dynein and kinesin in rat testis. Biol. Reprod 1992;46:817–828. [PubMed: 1534261]

Hayasaka S, Terada Y, Suzuki K, Murakawa H, Tachibana I, Sankai T, Murakami T, Yaegashi N, Okamura K. Intramanchette transport during primate spermiogenesis: expression of dynein, myosin Va, motor recruiter myosin Va, VIIa-Rab27a/b interacting protein, and Rab27b in the manchette during human and monkey spermiogenesis. Asian. J. Androl 2008;10:561–568. [PubMed: 18478159]

Held T, Paprotta I, Khulan J, Hemmerlein B, Binder L, Wolf S, Schubert S, Meinhardt A, Engel W, Adham IM. Hspa4l-deficient mice display increased incidence of male infertility and hydronephrosis development. Mol. Cell. Biol 2006;26:8099–8108. [PubMed: 16923965]

Huang Z, Khatra B, Bollen M, Carr DW, Vijayaraghavan S. Sperm PP1gamma2 is regulated by a homologue of the yeast protein phosphatase binding protein sds22. Biol. Reprod 2002;67:1936–1942. [PubMed: 12444072]

Hussey AJ, Hayes JD. Human Mu-class glutathione S-transferases present in liver, skeletal muscle and testicular tissue. Biochim. Biophys. Acta 1993;1203:131–141. [PubMed: 8218382]

Imai J, Maruya M, Yashiroda H, Yahara I, Tanaka K. The molecular chaperone Hsp90 plays a role in the assembly and maintenance of the 26S proteasome. EMBO J 2003;22:3557–3567. [PubMed: 12853471]

Junco A, Bhullar B, Tarnasky HA, van der Hoorn FA. Kinesin Light-Chain KLC3 expression in testis is restricted to spermatids. Biol. Reprod 2001;64:1320–1330. [PubMed: 11319135]

Kanai Y, Okada Y, Tanaka Y, Harada A, Terada S, Hirokawa N. KIF5C, a novel neuronal kinesin enriched in motor neurons. J. Neurosci 2000;20:6374–6384. [PubMed: 10964943]

Kierszenbaum AL. Spermatid manchette: plugging proteins to zero into the sperm tail. Mol. Reprod. Dev 2001;59:347–349. [PubMed: 11468770]

Kierszenbaum AL. Intramanchette transport (IMT): Managing the making of the spermatid head, centrosome, and tail. Mol. Reprod. Dev 2002;63:1–4. [PubMed: 12211054]

Kierszenbaum AL, Rivkin E, Tres LL. The actin-based motor myosin Va is a component of the acroplaxome, an acrosome-nuclear envelope junctional plate, and of manchette-associated vesicles. Cytogenet. Genome Res 2003;103:337–344. [PubMed: 15051957]

Kierszenbaum AL, Rivkin E, Tres LL. Expression of Fer testis (FerT) tyrosine kinase transcript variants and distribution sites of FerT during the development of the acrosome-acroplaxome-manchette complex in rat spermatids. Dev. Dyn 2008;237:3882–3891. [PubMed: 18985748]

Ko MS, Kitchen JR, Wang X, Threat TA, Wang X, Hasegawa A, Sun T, Grahovac MJ, Kargul GJ, Lim MK, Cui Y, Sano Y, Tanaka T, Liang Y, Mason S, Paonessa PD, Sauls AD, DePalma GE, Sharara R, Rowe LB, Eppig J, Morrell C, Doi H. Large-scale cDNA analysis reveals phased gene expression patterns during preimplantation mouse development. Development 2000;127:1737–1749. [PubMed: 10725249]

Kubalak SW, Miller-Hance WC, O'Brien TX, Dyson E, Chien KR. Chamber specification of atrial myosin light chain-2 expression precedes septation during murine cardiogenesis. J. Biol. Chem 1994;269:16961–16970. [PubMed: 8207020]

Kubota H, Yokota S, Yanagi H, Yura T. Structures and co-regulated expression of the genes encoding mouse cytosolic chaperonin CCT subunits. Eur. J. Biochem 1999;262:492–500. [PubMed: 10336634]

Lange BM, Bachi A, Wilm M, Gonzalez C. Hsp90 is a core centrosomal component and is required at different stages of the centrosome cycle in Drosophila and vertebrates. EMBO J 2000;19:1252–1262. [PubMed: 10716925]

Larkin MA, Blackshields G, Brown NP, Chenna R, McGettigan PA, McWilliam H, Valentin F, Wallace IM, Wilm A, Lopez R, Thompson JD, Gibson TJ, Higgins DG. Clustal W and Clustal X version 2.0. Bioinformatics 2007;23:2947–2948. [PubMed: 17846036]

Liu H, Krizek J, Bretscher A. Construction of a GAL1-regulated yeast cDNA expression library and its application to the identification of genes whose overexpression causes lethality in yeast. Genetics 1992;132:665–673. [PubMed: 1468625]

López-Fernández L, del Mazo J. Characterization of genes expressed early in mouse spermatogenesis, isolated from a subtractive cDNA library. Mamm. Genome 1996;7:698–700. [PubMed: 8703127]

Manandhar G, Schatten H, Sutovsky P. Centrosome reduction during gametogenesis and its significance. Biol. Reprod 2005;72:2–13. [PubMed: 15385423]

Manandhar G, Sutovsky P, Joshi HC, Stearns T, Schatten G. Centrosome reduction during mouse spermiogenesis. Dev. Biol 1998;203:424–434. [PubMed: 9808791]

Matsuoka R, Yoshida MC, Furutani Y, Imamura S, Kanda N, Yanagisawa M, Masaki T, Takao A. Human smooth muscle myosin heavy chain gene mapped to chromosomal region 16q12. Am. J. Med. Genet 1993;46:61–67. [PubMed: 7684189]

McClintock TS, Glasser CE, Bose SC, Bergman DA. Tissue expression patterns identify mouse cilia genes. Physiol. Genomics 2008;32:198–206. [PubMed: 17971504]

Mishra S, Somanath PR, Huang Z, Vijayaraghavan S. Binding and inactivation of the germ cell-specific protein phosphatase PP1gamma2 by sds22 during epididymal sperm maturation. Biol. Reprod 2003;69:1572–1579. [PubMed: 12826576]

Mochida K, Tres LL, Kierszenbaum AL. Structural features of the 26S proteasome complex isolated from rat testis and sperm tail. Mol. Reprod. Dev 2000;57:176–184. [PubMed: 10984418]

Morfini G, Szebenyi G, Elluru R, Ratner N, Brady ST. Glycogen synthase kinase 3 phosphorylates kinesin light chains and negatively regulates kinesin-based motility. EMBO J 2002;21:281–293. [PubMed: 11823421]

Odet F, Duan C, Willis WD, Goulding EH, Kung A, Eddy EM, Goldberg E. Expression of the Gene for Mouse Lactate Dehydrogenase C (Ldhc) Is Required for Male Fertility. Biol. Reprod. 2008

Poruchynsky MS, Sackett DL, Robey RW, Ward Y, Annunziata C, Fojo T. Proteasome inhibitors increase tubulin polymerization and stabilization in tissue culture cells: a possible mechanism contributing to peripheral neuropathy and cellular toxicity following proteasome inhibition. Cell Cycle 2008;7:940–949. [PubMed: 18414063]

Rivkin E, Cullinan EB, Tres LL, Kierszenbaum AL. A protein associated with the manchette during rat spermiogenesis is encoded by a gene of the TBP-1-like subfamily with highly conserved ATPase and protease domains. Mol. Reprod. Dev 1997;48:77–89. [PubMed: 9266764]

Rivkin E, Kierszenbaum AL, Gil M, Tres LL. Rnf19a, a ubiquitin protein ligase, and Psmc3, a component of the 26S proteasome, Tether to the acrosome membranes and the head-tail coupling apparatus during rat spermatid development. Dev. Dyn 2009;238:1851–1861. [PubMed: 19517565]

Rogers SL, Karcher RL, Roland JT, Minin AA, Steffen W, Gelfand VI. Regulation of melanosome movement in the cell cycle by reversible association with myosin V. J. Cell Biol 1999;146:1265–1276. [PubMed: 10491390]

Saade M, Irla M, Govin J, Victorero G, Samson M, Nguyen C. Dynamic distribution of Spatial during mouse spermatogenesis and its interaction with the kinesin KIF17b. Exp. Cell Res 2007;313:614–626. [PubMed: 17196196]

Sakai I, Sharief FS, Li SS. Molecular cloning and nucleotide sequence of the cDNA for sperm-specific lactate dehydrogenase-C from mouse. Biochem. J 1987;242:619–622. [PubMed: 2439071]

Shohet RV, Conti MA, Kawamoto S, Preston YA, Brill DA, Adelstein RS. Cloning of the cDNA encoding the myosin heavy chain of a vertebrate cellular myosin. Proceeding of the National Academy of Science USAProc of the Natl Acad Sci U S A 1989;86:7726–7730.

Simeone M, Phelan SA. Transcripts associated with Prdx6 (peroxiredoxin 6) and related genes in mouse. Mamm. Genome 2005;16:103–111. [PubMed: 15859355]

Soues S, Kann ML, Fouquet JP, Melki R. The cytosolic chaperonin CCT associates to cytoplasmic microtubular structures during mammalian spermiogenesis and to heterochromatin in germline and somatic cells. Exp. Cell Res 2003;288:363–373. [PubMed: 12915127]

Spite M, Baba SP, Ahmed Y, Barski OA, Nijhawan K, Petrash JM, Bhatnagar A, Srivastava S. Substrate specificity and catalytic efficiency of aldoketo reductases with phospholipid aldehydes. Biochem. J 2007;405:95–105. [PubMed: 17381426]

Tanaka K, Tsurumi C. The 26S proteasome: subunits and functions. Mol. Biol. Rep 1997;24:3–11. [PubMed: 9228274]

Tovich PR, Sutovsky P, Oko RJ. Novel aspect of perinuclear theca assembly revealed by immunolocalization of non-nuclear somatic histones during bovine spermiogenesis. Biol. Reprod 2004;71:1182–1194. [PubMed: 15189827]

Vignali G, Lizier C, Sprocati MT, Sirtori C, Battaglia G, Navone F. Expression of neuronal kinesin heavy chain is developmentally regulated in the central nervous system of the rat. J. Neurochem 1997;69:1840–1849. [PubMed: 9349526]

Vijayaraghavan S, Stephens DT, Trautman K, Smith GD, Khatra B, da Cruz e Silva EF, Greengard P. Sperm motility development in the epididymis is associated with decreased glycogen synthase kinase-3 and protein phosphatase 1 activity. Biol. Reprod 1996;54:709–718. [PubMed: 8835395]

Walden PD, Cowan NJ. A novel 205-kilodalton testis-specific serine/threonine protein kinase associated with microtubules of the spermatid manchette. Mol. Cell. Biol 1993;13:7625–7635. [PubMed: 8246979]

Walden PD, Millette CF. Increased activity associated with the MAST205 protein kinase complex during mammalian spermiogenesis. Biol. Reprod 1996;55:1039–1044. [PubMed: 8902215]

Wang R, Sperry AO. Identification of a novel leucine-rich repeat protein and candidate PP1 regulatory subunit expressed in developing spermatids. BMC Cell Biol 2008;9:9. [PubMed: 18237440]

Xia C, Rahman A, Yang Z, Goldstein LS. Chromosomal localization reveals three kinesin heavy chain genes in mouse. Genomics 1998;52:209–213. [PubMed: 9782088]

Yaffe MB, Farr GW, Miklos D, Horwich AL, Sternlicht ML, Sternlicht H. TCP1 complex is a molecular chaperone in tubulin biogenesis. Nature 1992;358:245. [PubMed: 1630491]

Yang J, Morales CR, Medvedev S, Schultz RM, Hecht NB. In the absence of the mouse DNA/RNA-binding protein MSY2, messenger RNA instability leads to spermatogenic arrest. Biol. Reprod 2007;76:48–54. [PubMed: 17035640]

Yang WX, Sperry AO. C-terminal kinesin motor KIFC1 participates in acrosome biogenesis and vesicle transport. Biol. Reprod 2003;69:1719–1729. [PubMed: 12826589]

Yoshida T, Ioshii SO, Imanaka-Yoshida K, Izutsu K. Association of cytoplasmic dynein with manchette microtubules and spermatid nuclear envelope during spermiogenesis in rats. J. Cell Sci 1994;107(Pt 3):625–633. [PubMed: 8006076]

Zhang, Y.; Wang, R.; Jefferson, H.; Sperry, AO. Identification of motor protein cargo by yeast 2-hybrid and affinity approaches. In: Sperry, AO., editor. Molecular Motors: Methods and Protocols. Vol. 392. Humana Press; Totowa, NJ: 2007. p. 97-116.

Zou Y, Millette CF, Sperry AO. KRP3A and KRP3B: candidate motors in spermatid maturation in the seminiferous epithelium. Biol. Reprod 2002;66:843–855. [PubMed: 11870094]

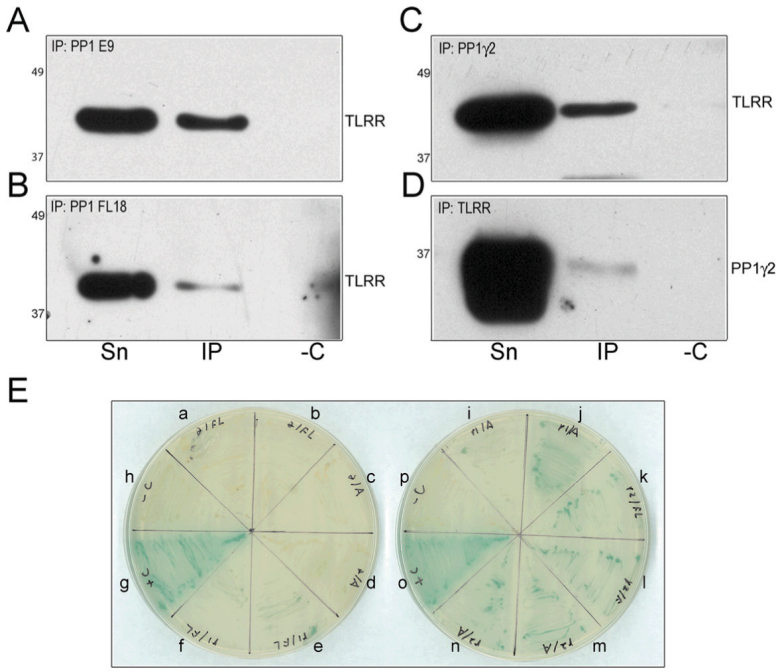

Figure 1. TLRR and PP1 interact in the testis

(A–D) Two pan-PP1 antibodies (PP1E9 and PP1FL18), a PP1 isoform specific antibody (anti-PP1γ2), or anti-TLRR were linked separately to Sepharose beads followed by incubation with 1.5–2 mg testis lysate. The antibody used for immunoprecipitation is indicated in the upper left-hand side of each panel: (A) PP1E9, (B) PP1FL18, (C) PP1γ2, and (D) TLRR. Unbound (Sn), or bound (IP) proteins were separated by PAGE, transferred to membrane and probed with antibodies to the proteins indicated at right. -C indicates proteins bound to Sepharose beads linked to normal rabbit IgG as a negative control. The migration of Benchmark prestained protein size standards (Invitrogen; Carlsbad, CA) is indicated to the left of each panel. (E) Yeast 2-hybrid interaction assay between TLRR and PP1 isoforms. TLRR, either full-length (TLRRFL) or a N-terminal fragment (TLRRA), and either PP1α, PP1γ1 or PP1γ2 were cotransformed into yeast strain YH109. Double transformants were selected on -LEU, -TRP plates and colonies streaked on indicator plates to detect induction of transcription from the LacZ and HIS3 genes. Double transformants shown are (a, b) TLRRFL+PP1α, (c, d) TLRRA +PP1α, (e, f) TLRRFL+PP1γ1, (i, j) TLRRA+PP1γ1, (k, l) TLRRFL+PP1γ2 (m, n), TLRRA +PP1γ2. Positive and negative controls for interaction are shown in (g, o) and (h, p), respectively.

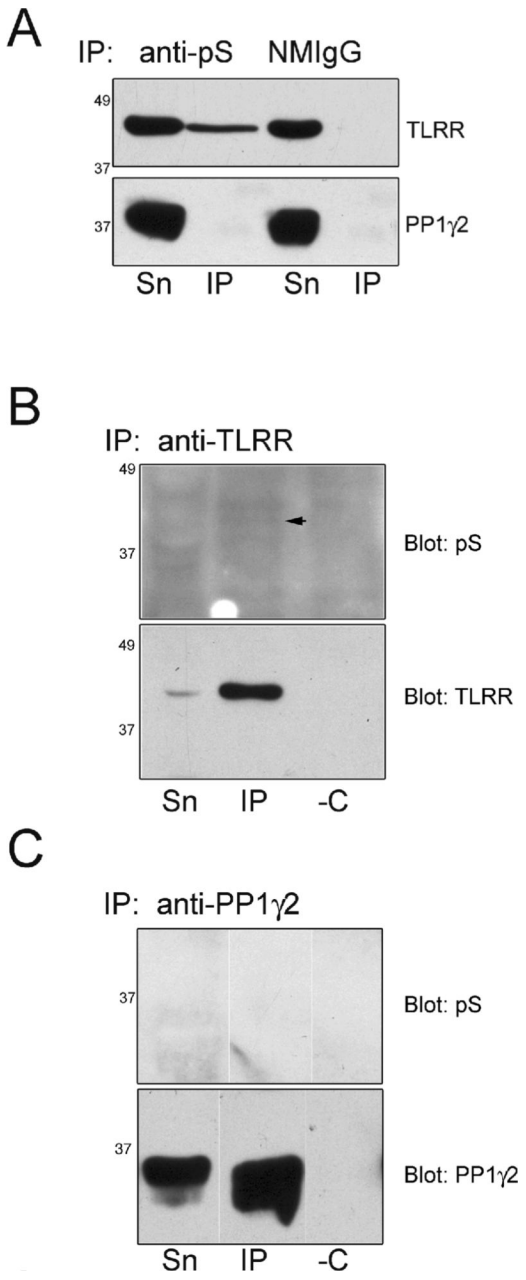

Figure 2. TLRR is likely a phosphoprotein

(A) A mixture of mouse antiphosphoserine antibodies (anti-pS) was linked to Sepharose beads according to the procedure described in Materials and Methods. Normal mouse IgG (NMIgG) was linked to beads and used as negative control for immunoprecipitation. The specificity of the antibody linked to beads is indicated at the top of the panel. Antibody-linked beads were incubated with 1.5–2 mg testis lysate and unbound (Sn) or bound (IP) proteins were separated by PAGE, transferred to membrane and probed with the TLRR antibody (upper panel) or the PP1γ2 antibody (lower panel). (B) The TLRR antibody bound to Sepharose beads, or (C) the PP1γ2 specific antibody linked to beads, was incubated with 1.5–2 mg testis lysate. Proteins unbound (Sn) or bound to the beads (IP) were separated by SDS-PAGE, transferred to membrane, and probed first with the anti-phosphoserine antibody (pS), stripped, and reprobed with the immunoprecipitating antibody to confirm immunoprecipitation. The arrow in B

indicates a phosphorylated protein in the bound fraction of the TLRR IP of about the same size as TLRR. PP1γ2 does not react with the anti-phosphoserine antibody. The migration of Benchmark prestained protein size standards (Invitrogen; Carlsbad, CA) is indicated at left.

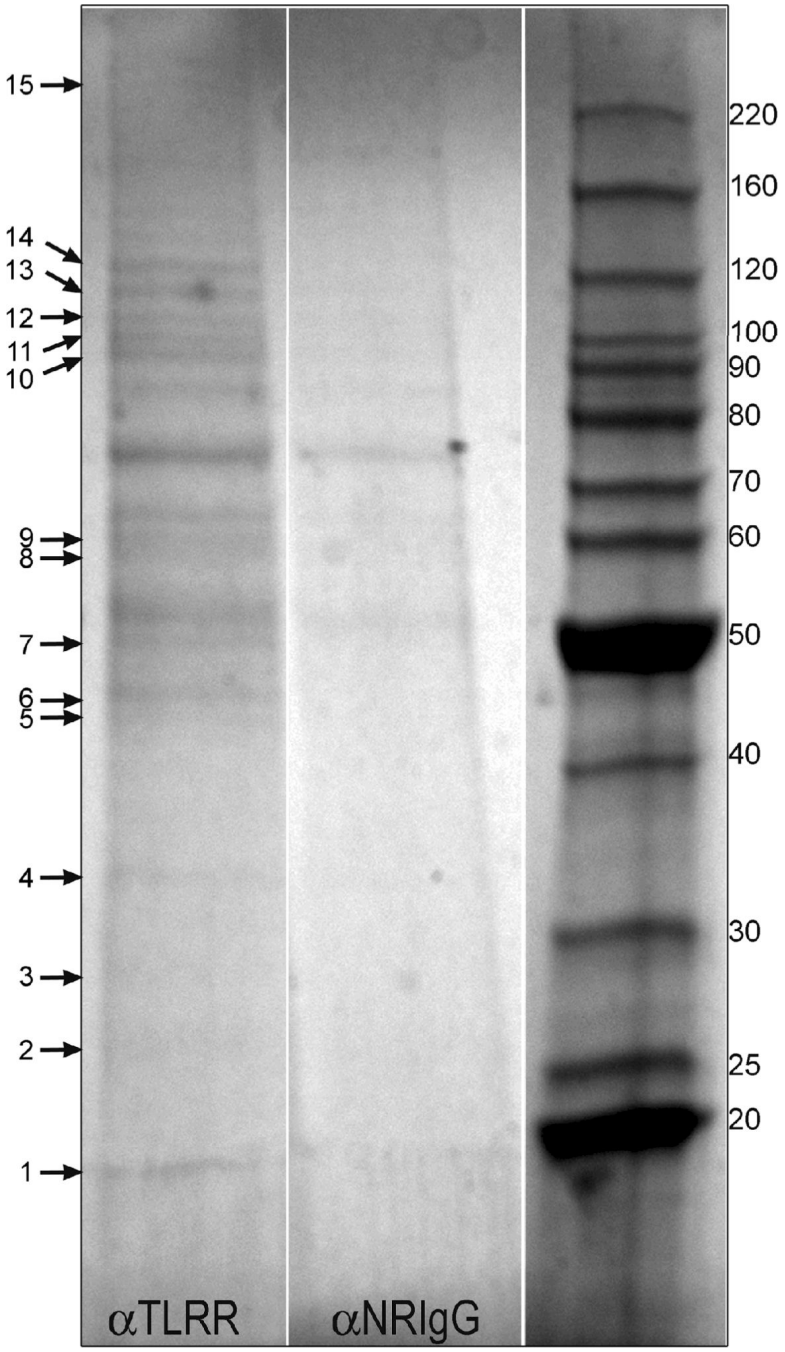

Figure 3. TLRR is part of a protein complex in the testis containing cytoskeletal proteins, chaperones, and components of the protein degradation pathway

An immunoaffinity column was prepared as described in Materials and Methods and used to purify TLRR and associated proteins from mouse testis lysate. A parallel column was also prepared linked to normal rabbit IgG (NRIgG) as a negative control. Eluates from both columns were concentrated, separated by SDS-PAGE, and stained with Coomassie R-250. All samples displayed were separated on the same gel. The 15 bands excised for sequencing and identification are numbered at left and correspond to the numbers listed in Table 1A, B, and C. The migration of Benchmark unstained protein size standards (Invitrogen; Carlsbad, CA) is indicated at right. This experiment was repeated 3 times resulting in an identical pattern of

TLRR-bound proteins, however, the resolution of the high molecular weight band 15 varied with experiment.

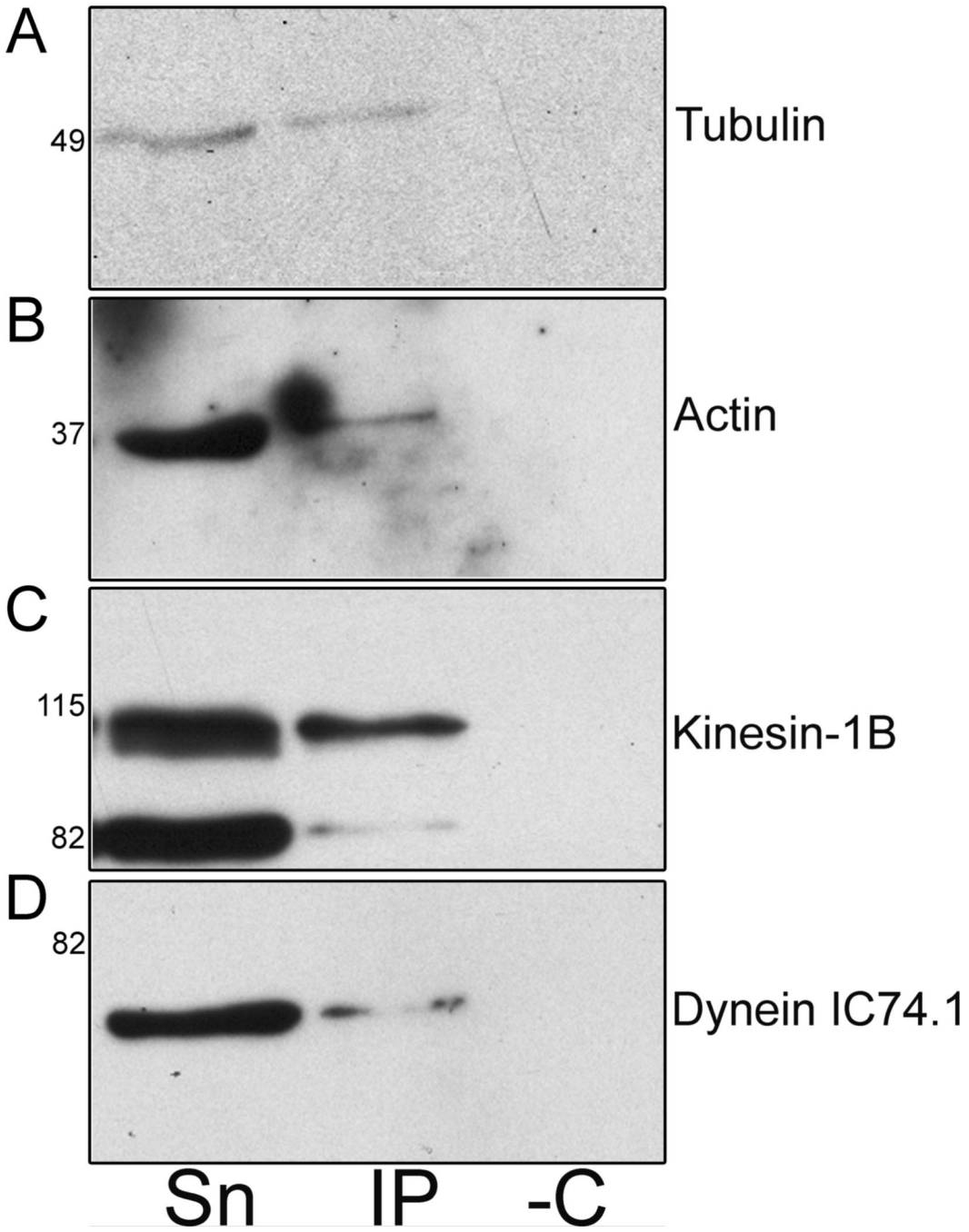

Figure 4. TLRR interacts with cytoskeletal polymer subunits and molecular motors

The affinity purified TLRR antibody bound to Sepharose beads, or nonspecific normal rabbit IgG (-C), was incubated with 1.5–2 mg testis lysate. Proteins unbound (Sn) or bound to the beads (IP) were separated by SDS-PAGE, transferred to membrane, and probed with antibodies to the proteins indicated at right: (A) tubulin, (B) actin, (C) kinesin-1B, and (D) dynein IC 74.1. The migration of Benchmark prestained protein size standards (Invitrogen; Carlsbad, CA) is indicated at left.

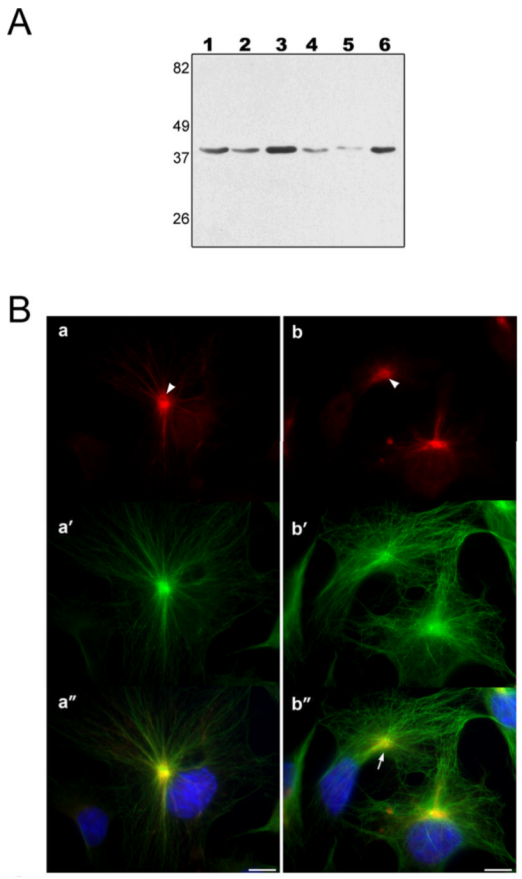

Figure 5. TLRR is expressed in cultured cells and closely aligns with the microtubule cytoskeleton

(A) Protein extracts were made from either mouse testis (lane 1) or cultured cells (lanes 2, COS7; 3, MCF7; 4, DU145; 5, 10T½; 6, NIH 3T3). 100 μg protein was loaded per well, separated by electrophoresis, transferred to membrane and probed with the TLRR antibody. The migration of Benchmark prestained protein size standards (Invitrogen; Carlsbad, CA) is indicated to the left. (B) Two examples of TLRR colocalization with microtubules are shown (a-a″ and b-b″). COS7 cells were grown to approximately 70% confluency, fixed and double-stained with the TLRR antibody (panels a and b, red) and an antibody to α-tubulin (panel a′ and b′, green). Arrowheads in panels a and b indicate loops of TLRR antibody stained material near the MTOC while the arrow in panel b″ indicates the MTOC displaced from the nucleus in a putative motile cell. Signal from the 2 channels, including the blue channel (DNA, DAPI) was merged in panels a″ and b″. The bar indicates 10μm.

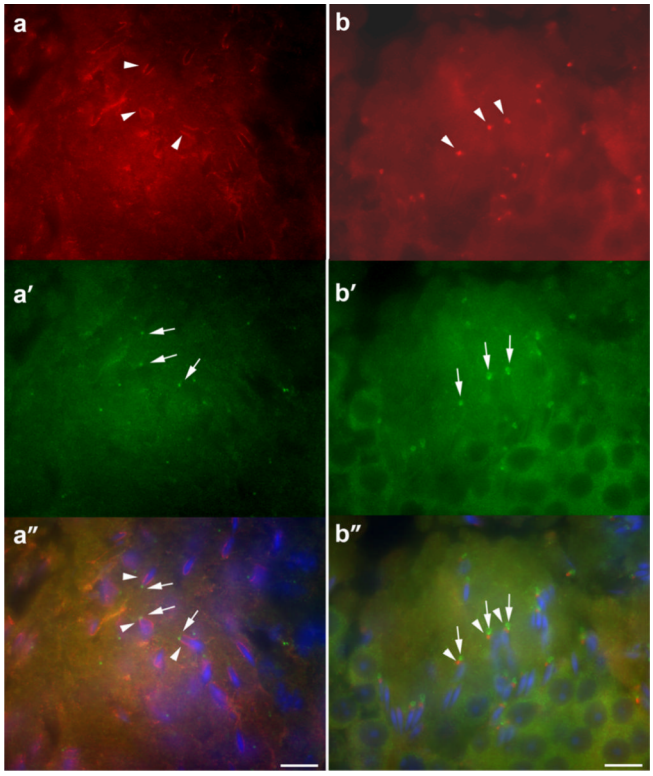

Figure 6. TLRR localizes to the centrosomal region of late stage spermatids

Testis sections were triple-stained with antibodies against TLRR (panels a and b, red), γ-tubulin (panels a′ and b′, green), and DAPI (panels a″ and b″, blue). Panels a" and b″ represent the merged image from all three channels. TLRR staining in midstage spermatids (arrowheads a and a″) does not align with that of γ-tubulin (arrows, a′ and a″). However, in later stage spermatids, TLRR (arrowheads, b and b″) and γ-tubulin (arrows, b′ and b″) are found adjacent to one another in the centrosomal region at the base of the sperm head. The bar indicates 10μm.

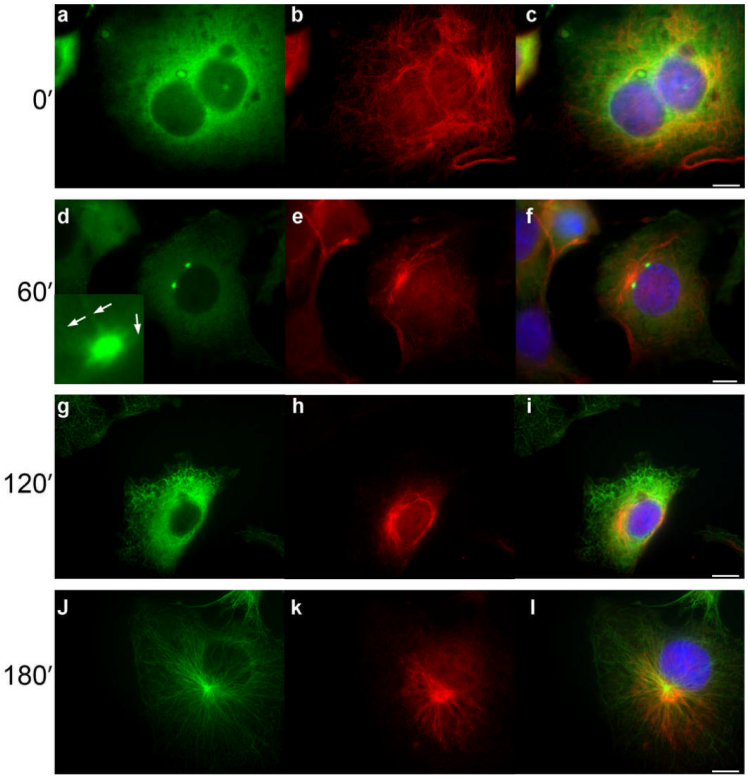

Figure 7. TLRR localization does not depend entirely on microtubules

COS7 cells were treated with 25 μM nocodazole for 1.5 hours, allowed to recover from drug treatment for 0, 1, 2, or 3 hours, fixed and double-stained with anti α-tubulin (a, d, g, j) and TLRR antibody (b, e, h, k). Respective merged channels for each time point are shown in panels c, f, i, and l. The bar indicates 10μm.

Table 1A

Cytoskeletal components

Protein Name	band#	Protein ID	#peptides identified	% sequence coverage	comments/references
myosin regulatory light chain Myl9	1	gi|198278553	6	45	(Kubalak et al., 1994)
β–actin	5	Q3UAF7	13	42	(Cleveland et al., 1980)
Kinesin family member 5B	14	Q5BL10	25	29	(Xia et al., 1998)
γ–actin	1	gi|950002	10	27	(Cleveland et al., 1980)
smooth muscle myosin Myh11	15	gi|50510675	42	25	(Matsuoka et al., 1993)
β–Tubulin	7	Q99JZ6	10	24	(Cleveland et al., 1980)
non-muscle myosin Myh10	15	gi|33598964	34	21	(Eddinger and Wolf, 1993)
α–actin	1	gi|49870	6	18	(Cleveland et al., 1980)
non-muscle myosin Myh9	15	gi|114326446	29	18	(Shohet et al., 1989)

Table 1B

Protein stability

Protein Name	band#	Protein ID	#peptides identified	% sequence coverage	comments/references
Psmd3, 26S proteasome non-ATPase subunit 3	8	PSD3_mouse	11	32	(Tanaka and Tsurumi, 1997) manchette associated (Rivkin et al., 1997)
Heat shock protein 90α	10	HS90A	23	29	highly expressed in testis (Gruppi et al., 1991) proteasome stabilization (Imai et al., 2003)
Psmd1, proteasome 26S non-ATPase subunit 1	13	BAE31950	19	25	(Tanaka and Tsurumi, 1997) manchette associated (Rivkin et al., 1997)
Psmd2 proteosome 26S non ATPase subunit 2	11	Q3TWL6	21	24	(Tanaka and Tsurumi, 1997) manchette associated (Rivkin et al., 1997)
Heat shock protein 90β	12	Q91V38	18	22	(Gruppi et al., 1991)
CCT (chaperonin containing TCP-1), theta chain	8	JC4073	9	18	tubulin/actin folding (Gao et al., 1992; Yaffe et al., 1992) manchette associated (Soues et al., 2003)
CCT, gamma chain	9	S43062	10	18	tubulin/actin folding (Gao et al., 1992; Yaffe et al., 1992) manchette associated (Soues et al., 2003)
heat shock protein 4-like	12	AAC52610	14	17	required for spermatogenesis (Held et al., 2006)
VCP, valosin containing protein, AAA ATPase p97	11	S25197	12	14	ubiquitin pathway (Dai and Li, 2001)
CCT, zeta chain	8	Q52KG9	5	9	tubulin/actin folding (Gao et al., 1992; Yaffe et al., 1992) manchette associated (Soues et al., 2003)

Table 1C

Miscellaneous enzymes and other proteins

Protein Name	band#	Protein ID	#peptides identified	% sequence coverage	comments/references
glutathione-S-transferase mu 1	2	gi|6754084	10	49	metabolism (Hussey and Hayes, 1993)
peroxiredoxin 6	2	gi|6671549	7	41	metabolism (Simeone and Phelan, 2005)
enoyl coexzyme A hydratase	3	gi|148685962	8	40	(Ko et al., 2000)
Lactate dehydrogenase c	4	Q64483	9	30	metabolism, testis specific isoform, postmeiotic germ cells, required for fertility (Sakai et al., 1987; Odet et al., 2008)
albumin 1	9	Q546G4	13	21	
MSY2	6	CAI35155	8	20	germ cell specific, mRNA stability, required for spermatogenesis (Gu et al., 1998) (Yang et al., 2007)
aldose reductase	5	gi|786001	4	12	metabolism (Spite et al., 2007)
Ilf2, interleukin enhancer binding factor 2	6	Q3UXI9	4	10	transcription, male/female germ cells (López-Fernández and del Mazo, 1996)